Chemical Physics Letters 586 (2013) 21–28

Contents lists available at ScienceDirect

Chemical Physics Letters

journal homepage: www.elsevier.com/locate/cplett

Ionization/dissociation processes of methyl-substituted derivates of cyclopentanone in intense femtosecond laser field

Qiaoqiao Wang [a,1], Yuri A. Dyakov [b], Di Wu [a], Dongdong Zhang [a], Mingxing Jin [a], Fuchun Liu [a], Hang Liu [a], Zhan Hu [a], Dajun Ding [a,*], Hirobumi Mineo [c], Yoshiaki Teranishi [d], Sheng Der Chao [c], Sheng Hsien Lin [a,d], O.K. Kosheleva [e], A.M. Mebel [f,*]

[a] Institute of Atomic and Molecular Physics, Jilin University, Changchun 130012, PR China
[b] Institute of Atomic and Molecular Sciences, Academia Sinica, Taipei 106, Taiwan
[c] Institute of Applied Mechanics, National Taiwan University, Taipei 106, Taiwan
[d] Department of Applied Chemistry, National Chiao-Tung University, Hsin-Chu 300, Taiwan
[e] Genomic Research Center, Academia Sinica, Taipei 115, Taiwan
[f] Department of Chemistry and Biochemistry, Florida International University, 11200 SW 8th Street, Miami, FL 33199, USA

ARTICLE INFO

Article history:
Received 30 June 2013
In final form 3 September 2013
Available online 8 September 2013

ABSTRACT

Ionization and dissociation of 2- and 3-methyl cyclopentanones have been investigated in molecular beams by their irradiation with intense 394 and 788 nm laser fields with pulse duration of 90 fs and intensity of 3×10^{13}–4×10^{14} W/cm^2. The analysis of the resulting mass spectra allowed us to discern the effects of methyl substitution and its position on the outcome of ionization/dissociation processes induced by the intense femtosecond laser field. Generalized Keldysh-Faisal-Reiss (g-KFR) and *ab initio* G3(MP2,CCSD)//B3LYP/6–31G*/RRKM theoretical calculations helped to uncover the formation mechanism of major ionic fragments observed in the mass spectra including $C_5H_{10}^+$, $C_4H_6O^+$, $C_3H_3O^+$, $C_3H_4O^+$, $C_3H_x^+$, and $C_2H_x^+$.

1. Introduction

Unsaturated aliphatic cycloketones are well-known for their flexible structures [1] and their spectra were investigated by various experimental methods, including low-energy electron impact ionization [2] and resonance enhanced multiphoton ionization [3–5]. Photodissociation mechanisms of the neutral molecules were proposed based on these studies. In 2000–2002, Zewail and co-workers studied evolution of reaction intermediates for a series of cycloketones by using the femtosecond pump–probe method providing a real-time picture of the nuclear motions and structural changes during the reaction [6,7]. A subsequent study of cyclopentanone and cyclohexanone in intense femtosecond laser fields indicated that their fragmentation was enhanced with the laser intensity and molecular size [8]. Previously, we interpreted dissociation patterns of cycloketones based on the cation absorption at the laser wavelength using experimental measurements combined with time-dependent density functional theory calculations of the molecular absorption spectra [9]. Thereafter, we investigated the dynamic processes of cyclopentanone in 90 fs laser fields. We compared the ion yield of the parent ion by experimental measurements and g-KFR calculations and discussed the dissociation pattern based on RRKM theory and *ab initio* calculations [10].

In the present Letter, we consider 2- and 3-methyl-substituted cyclopentanones affording an opportunity to compare the behavior of a cycloketone with and without an out-of-ring substituent group and with the substituent in different positions in the photoionization and photodissociation processes in intense femtosecond laser field. Methylation may differently affect various molecular properties. Particularly, it was established that the lowest singlet and triplet $\pi \rightarrow \pi^*$ states of some amino acids are insensitive to methylation, while the $^1(n \rightarrow \pi^*)$ and $^1(n \rightarrow R)$ excitations are sensitive [11]. Photodissociation reactions of *N*-methylindole, *N*-methylpyrrole, and anisole were found to be not sensitive to methylation in excited electronic states, but have quite different product distributions in the ground state when compared to unsubstituted indole, pyrrole and phenol [12]. Dissociation of toluene [13] and 4-methylpyridine [14] in the ground electronic state was found to occur through a seven-membered ring intermediate and to have different product branching ratios as compared to benzene and pyridine, respectively. Properties of methylated uracil [15] and linear hydrocarbons [16] strongly depend on the methyl group position. Generally, methylation of organic molecules modifies their chemical and electronic properties due to changes both in the geometry and the electronic structure. In this Letter, we discuss the methylation

* Corresponding authors. Fax: +86 431 8516 8816 (D. Ding); +1 305 348 3772 (A.M. Mebel).
E-mail addresses: dajund@jlu.edu.cn (D. Ding), mebela@fiu.edu (A.M. Mebel).
[1] The present address: Institute of Theoretical Physics, Chinese Academy of Sciences, Beijing 100190, PR China.

0009-2614/$ - see front matter © 2013 Elsevier B.V. All rights reserved.
http://dx.doi.org/10.1016/j.cplett.2013.09.009

effect on the behavior of cyclopentanone in intense femtosecond laser field.

Experimentally, we use 394 and 788 nm fs laser pulses to irradiate methyl-substituted cyclopentanones and to observe ion signals with a time-of-flight mass spectrometer (TOF-MS). Theoretically, we perform calculations of ionization rate constants for the molecules utilizing g-KFR theory. A qualitative analysis of the dissociation mechanism after the femtosecond laser pulse irradiation have been performed using RRKM theory based on *ab initio* potential energy surfaces (PES).

2. Experimental and theoretical methods

2.1. Experimental setup

The experimental setup utilized in the present fs laser ionization and dissociation study has been introduced in detail previously [9,10,17]. All experiments were performed using a time-of-flight mass spectrometer (TOF-MS) combined with a chirped pulse amplifier (CPA) Ti: sapphire laser (TSA, Spectra-Physics). The linearly polarized output laser pulse, centered at 788 nm, has a pulse width of 90 fs (FWHM), and repetition rate of 10 Hz. A BBO crystal was used to generate a frequency doubled laser beam (wavelength centered at 394 nm). The laser beam was focused using a quartz plano-convex lens (f = 350 mm) and entered the vacuum chamber via a quartz window. The intensity of the laser beam was attenuated by using a rotatable half-wave plate followed by a Glan–Taylor prism and has been varied in the range from 10^{13} to 10^{14} W/cm^2, which was estimated based on a number of parameters including the energy per pulse, the pulse width, the mirror focal length, laser wavelength, and the pre-focused beam diameter.

Liquid samples of cyclopentanone (C_5H_8O), 2-methyl-cyclopentanone ($C_6H_{10}O$) and its isomer (3-methyl-cyclopentanone, $C_6H_{10}O$) from Aldrich Co. Ltd. (purity >99%) were used without further purification. The Argon carrier gas with the sample vapor (the ratio is 100/1) was expanded through the pulsed nozzle (400 μs duration) into the vacuum chamber through a skimmer. A home-made mass spectrometer, operating on Wiley–McLaren focusing conditions, was employed to measure the mass distribution of ions produced by the laser beam. The mass resolution at m/e = 100 is $M/\Delta M$ = 1000. A slit of 0.5 mm width was located on the extraction plate. The pressure of the vacuum chamber was maintained in the order of 10^{-5} Pa during experiments. The produced ions were finally detected by a dual microchannel plate (MCP) detector placed at the end of the mass spectrometer. All mass spectra used in this Letter were obtained by accumulating and averaging over 512 laser shots.

2.2. Generalized KFR calculations

Earlier [10], we investigated the photoionization mechanisms of cyclopentanone with the same experimental setup. By comparing the experimental results with theoretical ionization rates computed utilizing ADK [18,19], Keldysh [20–22], KFR [23–26], and generalized KFR (g-KFR) theories [27], we concluded that the g-KFR theory was the most suitable method to calculate the ionization rate of cyclopentanone. It should be noted that the original Keldysh theory (KFR) was developed for atoms, especially one-electron atoms. Our group modified this theory so that it can be applied to treat molecules, which are multi-centered (that is, consist of multi-nuclei and usually multi-electrons). For this purpose we use the Born–Oppenheimer adiabatic approximation and compute the electronic structure based on the molecular orbital theory. This modification was called generalized Keldysh theory, or g-KFR theory [21,22,27,28]. Accordingly, in the present Letter we choose the g-KFR theory to analyze the photoionization of 2- and 3-methyl-cyclopentanones because the electronic structures of these two compounds should be similar to that of cyclopentanone.

Briefly, in g-KFR theory, the ground electronic state of a molecule (or a molecular cation) is assumed to be well described in terms of molecular orbitals obtained from *ab initio* calculations. The ionized electron wave function is described by the Volkov continuum state. Then, the photoionization rate can be computed on the assumption that the ionization only takes place from the highest occupied molecular orbital (HOMO) [27–29]. The sequential ionization process is supposed to be the main channel for producing multi-charged molecular ions. Then, the averaged ionization yield can be evaluated by solving the rate equation and taking into account the Gaussian shape of the spatial and time distributions of the laser pulse [22,30,31]. Previous applications [10,17,31] confirmed g-KFR theory to be suitable for calculations of molecular ionization rates.

2.3. Ab initio/RRKM calculations

We assume here that the fragmentation occurs by the ionization followed by dissociation (ionization–dissociation) mechanism. This assumption is justified because, first, the rate of the electron motion is faster than that for the nuclear motion, and second, if neutral dissociation takes place, the molecule first has to absorb energy from the laser and then to either pre-dissociate or to decompose after internal conversion. The neutral fragments produced would be ionized afterwards. It is common that such processes take place on a picosecond timescale or even slower, which is longer than the laser pulse duration of ~100 fs, and hence this dissociation-ionization mechanism is rather unlikely.

Therefore, we performed *ab initio* quantum chemical calculations of PES of the 2- and 3-methyl-cyclopentanone ions. The density functional B3LYP/6–31G* method [32] was used to perform geometry optimizations and single-point energies were refined by G3(MP2,CCSD) *ab initio* calculations [33,34]. All *ab initio* calculations were performed using the Gaussian 03 [35] and Molpro 2002 packages [36]. The computed frequencies and energies of the intermediates and transition states were utilized for microcanonical RRKM calculations of energy-dependent reaction rate constants using the formalism described in our previous works [10,17,31,37,38].

It is important to address the applicability of this statistical approach for describing the ionization–dissociation mechanism. The first issue concerns with the total amount of internal energy E accumulated by a molecule during the excitation–ionization process. In photodissociation molecular beam experiments, where photoexcitation to an electronically excited state is followed by relaxation to the ground state through internal conversion, the value of E is typically equal to the energy of the absorbed photon. Then, energy-dependent RRKM rate constants can be computed and product branching ratios derived from these rate constants are capable to closely describe experimental data measured under single-collision conditions, i.e., at the zero-pressure limit [39–43]. To estimate the internal energy E for multi-photon ionization-dissociation reactions, one needs to know the number of photons absorbed by a molecule and the translational energy of emitted electrons; otherwise, we can only consider a wide range of E. This problem was discussed earlier in relation to the dissociative ionization of methane in intense femtosecond laser field [31] and it was concluded that the parent ions are produced with a wide distribution of internal energies. This makes the microcanonical RRKM calculations a

qualitative tool for understanding reaction mechanisms leading to various product ions rather than a quantitative method for accurately evaluating product branching ratios. Second, it is impossible to estimate the internal energy of daughter fragments produced by dissociation of the parent ion. The internal energy of secondary fragments should be lower than the energy of the parent ion because of energy redistribution among vibrational, translational, and rotational degrees of freedom of products. Thus, in the present Letter we confine ourselves to a qualitative analysis of secondary reactions and do not calculate their product branching ratios due to the uncertainty in the internal energies and the complicated dissociation scheme of the parent ion.

Third, at high internal vibrational energies the RRKM calculated rate constants may exceed the applicability limit of RRKM theory, which normally is assumed to be $10^{13}\,s^{-1}$ – the typical rate of intramolecular vibrational redistribution (IVR). Therefore, the behavior of the system at high internal energies can deviate from the statistical (RRKM) behavior. Keeping these three points in mind, we emphasize that the results of our *ab initio*/RRKM calculations only provide a qualitative guide on the formation mechanisms of various products and their relative importance.

3. Results and discussions

3.1. Ionization processes of 2- and 3-methyl-cyclopentanones and cyclopentanone in various laser fields

The Keldysh parameter γ [20], related to the laser frequency and ionization potential of the compounds under consideration, usually acted as a qualitative criterion characterizing the ionization processes. The multiphoton ionization (MPI) plays an important role if $\gamma \gg 1$, whereas tunneling ionization (TI) occurs if $\gamma \ll 1$. The ionization potential of 2-methyl-cyclopentanone is 9.08 eV [44] and, when the laser wavelength is 394 nm, a simple evaluation indicates that the laser intensity tends to $3.1 \times 10^{14}\,W/cm^2$ if $\gamma \sim 1$. For 788 nm, the critical laser intensity tends to $7.8 \times 10^{13}\,W/cm^2$. Likewise, the ionization potential of 3-methyl-cyclopentanone is 9.20 eV [44], and the estimated critical laser intensity is 3.2×10^{14} and $7.9 \times 10^{13}\,W/cm^2$ for 394 and 788 nm, respectively.

The experimental ion yields of 2- and 3-methyl-cyclopentanones as functions of the laser intensity from 2×10^{13} and 3×10^{14} W/cm^2 are plotted in the log–log form in Figure 1, panels a–d, for different wavelengths. Here, the ion yields are determined from the ion peak area below the curves in the measured mass

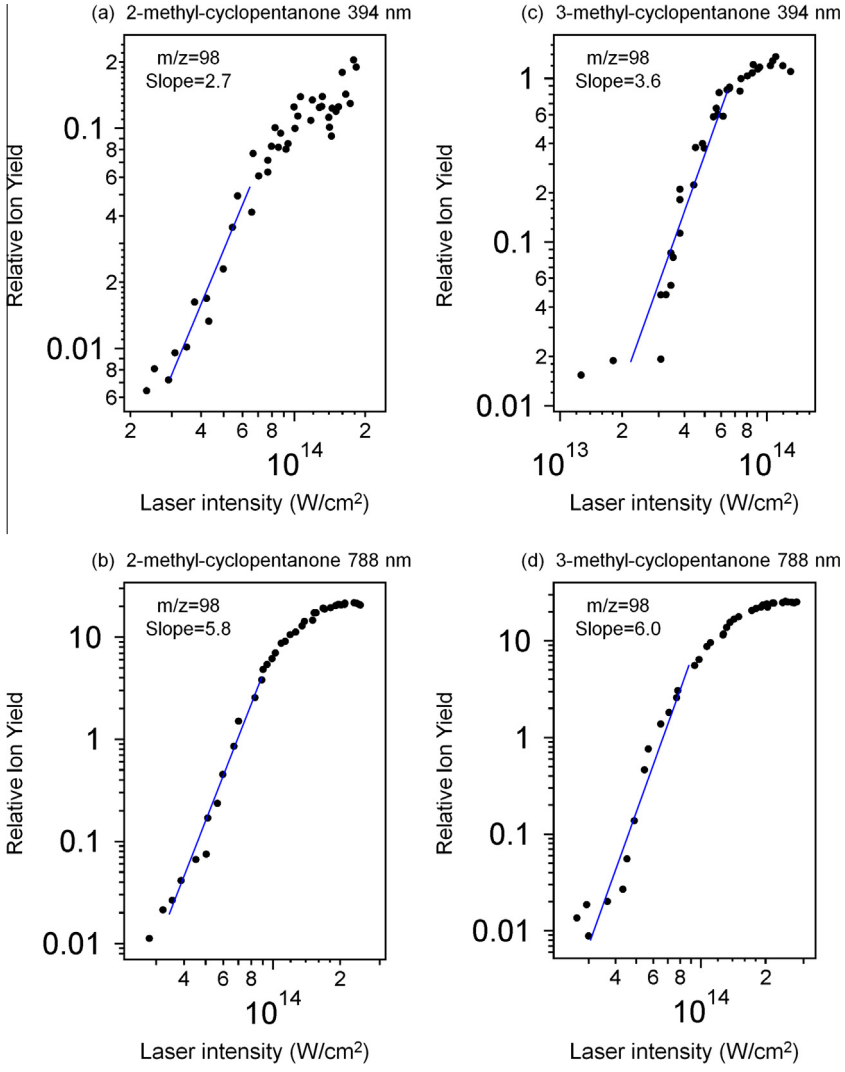

Figure 1. Experimental ion yields of 2-, 3-methyl-cyclopentanone parent ions as a function of laser intensity, ranging from 2×10^{13} to $3 \times 10^{14}\,W/cm^2$. The wavelengths are 394 nm (a and c) and 788 nm (b and d). A linear fit through the data points is shown as the solid blue line. (For interpretation of the references to colour in this figure legend, the reader is referred to the web version of this article.)

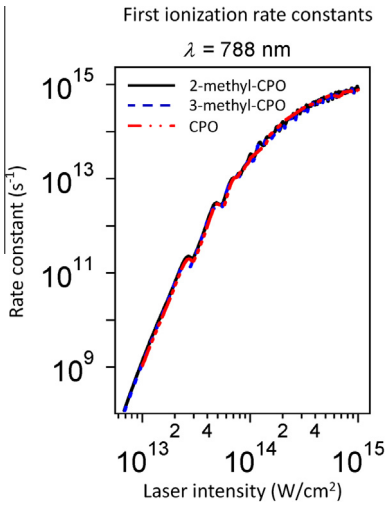

Figure 2. First ionization rate constants of 2-methyl-cyclopentanone (2-methyl-CPO, black solid line), 3-methyl-cyclopentanone (3-methyl-CPO, blue dashed line), and cyclopentanone (CPO, red dotted lines) calculated using g-KFR theory at $\lambda = 788$ nm. (For interpretation of the references to colour in this figure legend, the reader is referred to the web version of this article.)

spectrum. As the absorbed energy required for the ionization process should be at least beyond the ionization potential energy of the compound (9.08 and 9.20 eV for 2- and 3-methyl-cyclopentanones, respectively), for the multiphoton ionization to occur, three or six laser photons are required for the 394 and 788 nm wavelengths, respectively. Take 2-methyl-cyclopentanone in the 394 nm laser field for example. According to the linear fit of the measured data points, the laser dependence of the observed parent ion yields roughly shows a power law of $\sim I^3$, that is, the slope of 3 in the log–log scale which corresponds to the minimal number of photons required for ionizing the molecule. Meanwhile, the ion yields of 2-methyl-cyclopentanone show a behavior of $\sim I^6$ for 788 nm, which also satisfies the requirement for the multiphoton ionization to occur. As about 3-methyl-cyclopentanone, we could obtain similar experimental results.

In Figure 2, the first photoionization rate constants of the 2- and 3-methyl-cyclopentanones as well as cyclopentanone obtained within the g-KFR theory [27–29] and using realistic molecular orbitals and the ionization potential energies are plotted in the log–log form as functions of the laser intensity for 788 nm. It is notable that the laser intensity dependences of the photoionization rate constants for these three compounds at a fixed wavelength exhibit similar trends. According to a linear fit of the calculated data under 1×10^{14} W/cm^2, the slopes of these three curves at 788 nm are nearly equal to six, which corresponds to the minimal number of photons needed to ionize these three compound via multiphoton ionization and is consistent with the experimental measurements.

As mentioned previously [10], the HOMO of a ketone molecule is a nonbonding orbital of the C–O group, which has a *p*-orbital character. Thus, it is reasonable that the position of the substituent may play only a small role in the ionization process. Considering that the ionization energies of the two methyl-substitute cyclopentanones and cyclopentanone are also close, it is logical to expect that the laser intensity dependences of the singly charged parent ions would exhibit similar trends.

A similar analysis could be used for the doubly charged parent ions. Based on our previous study [10], the second photoionization rate constants for cyclopentanone are much smaller (by a factor of 10^4 at 10^{15} W/cm^2) than those for the first photoionization. Therefore, the peak at $m/z = 42$ in the mass spectrum is more likely to be attributed to a fragment ion rather than to the doubly charged parent ion. In the present Letter, considering the similarity of molecular structures and ionization energies, we can also expect that the peaks at $m/z = 49$ in the mass spectra for 2- and 3-methyl-cyclopentanones are more likely to be originated from fragment ions which have the same mass-to-charge ratio as that for the doubly charge parent ions.

3.2. Dissociation processes of 2- and 3-methyl-cyclopentanones and cyclopentanone induced by various laser fields

When cyclopentanone and two structural isomers of methyl-cyclopentanone interacted with a 788 nm fs laser pulse at 3.5×10^{13} W/cm^2, the TOF mass spectra illustrated in Figure 3a

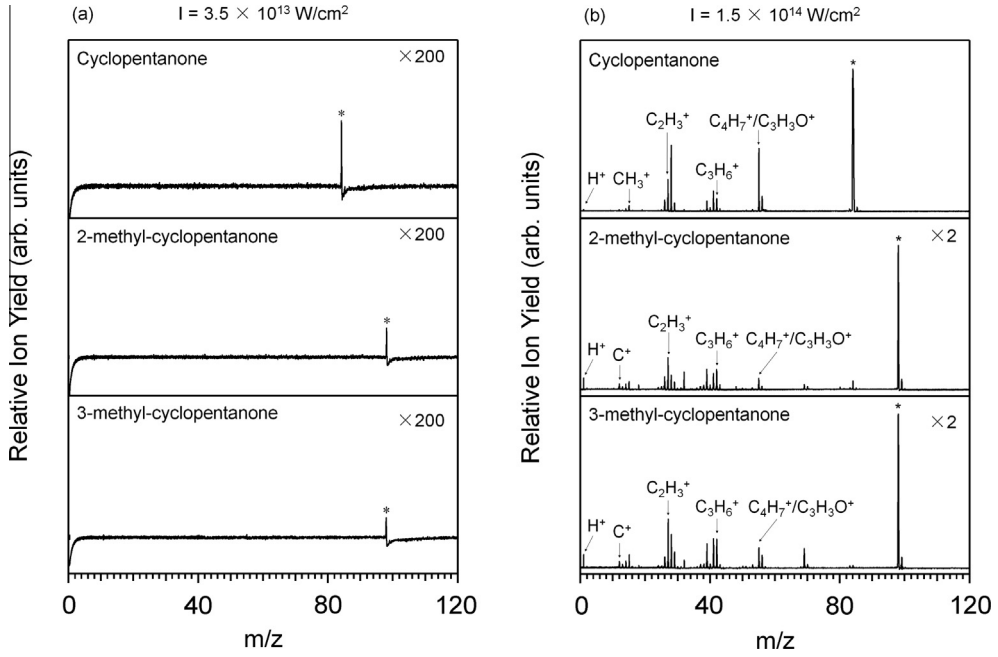

Figure 3. Mass spectra of cyclopentanone, 2-methyl-cyclopentanone and 3-methyl-cyclopentanone interacted with 90 fs laser pulses at 788 nm of different intensities: (a) 3.5×10^{13} W/cm^2; (b) 1.5×10^{14} W/cm^2. The asterisk denotes the parent ion.

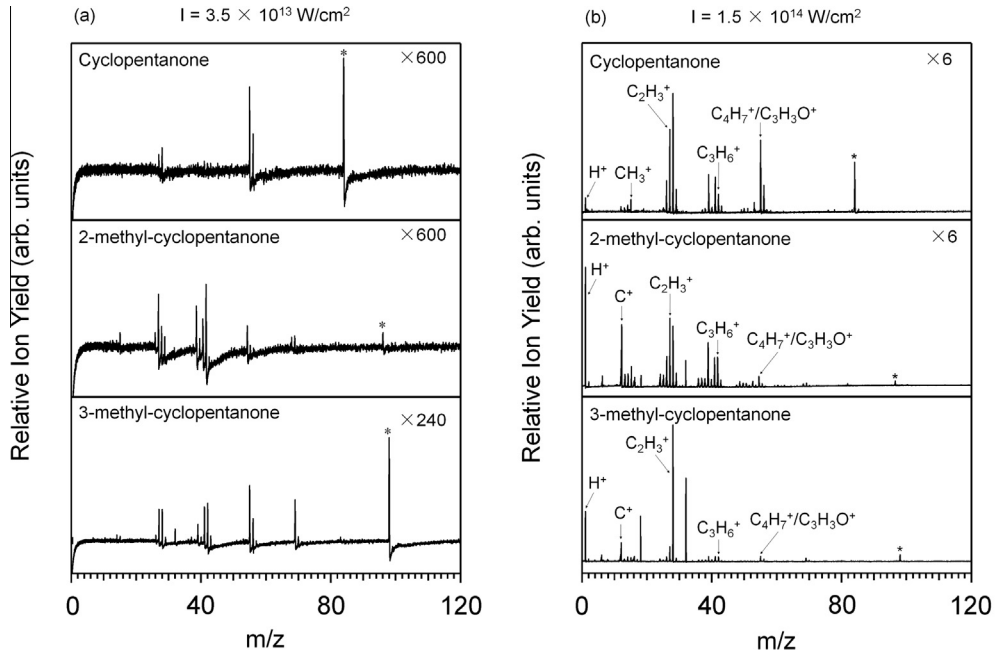

Figure 4. Mass spectra of cyclopentanone, 2-methyl-cyclopentanone and 3-methyl-cyclopentanone interacted with 90 fs laser pulses at 394 nm of different intensities: (a) 3.5×10^{13} W/cm^2; (b) 1.5×10^{14} W/cm^2. The asterisk denotes the parent ion.

were obtained. The parent ion peaks for all the three cycloketones denoted by the asterisk are dominant and are accompanied by weak peaks from fragment ions. With the increasing laser intensity, some large fragment ions appear first. When the laser intensity increases to 1.5×10^{14} W/cm^2, as shown in Figure 3b, the parent ions are still predominant in the mass spectra, however, the fragmentation is deeper and smaller fragments appear. On the contrary to the 788 nm case, all three compounds exhibit heavier fragmentation at 394 nm, as shown in Figure 4. Although the singly-charged parent ions are still predominant at lower laser intensities, we could clearly observe numerous fragment ions in the mass spectra. When the laser intensity increases, the peaks corresponding to the singly charged parent ions for all three compounds rapidly decrease, whereas those for the fragments rise.

The following fragment peaks can be observed in the mass spectra:

(1) m/z = 83 and 84 u. The 84 u peak is the parent ion in the case of cyclopentanone. For 2-methyl-cyclopentanone, a weak 83 u peak is present in the spectra at both wavelengths at the higher intensity, whereas for 3-methyl-cyclopentanone, only very weak 83 and 84 u peaks of approximately equal intensities can be seen only at 788 nm and 1.5×10^{14} W/cm^2. Apparently, these peaks can be assigned to $C_5H_7O^+$ and $C_5H_8O^+$.

(2) m/z = 69 and 70 u. These peaks are present both for 2- and 3-methyl-cyclopentanones at 788 nm, with the 69 u peak being more intense especially for 3-methyl-cyclopentanone. Very weak 69 u peaks can be seen at 394 nm. The peaks are completely absent for cyclopentanone. A tentative assignment could be $C_5H_9^+/C_4H_5O^+$ (69) and $C_5H_{10}^+/C_4H_6O^+$ (70).

(3) m/z = 48–56 u. Although this group of peaks can be found in almost all spectra, the 48–54 u peaks are usually weak or just above the noise. The strongest peak in the group is 55 u followed by 56 u, with a tentative assignment being $C_4H_7^+/C_3H_3O^+$ (55) and $C_4H_8^+/C_3H_4O^+$ (56). The remaining weak peaks in the series can be obtained by secondary consecutive H losses from $C_4H_7^+$ (down to C_4^+) and $C_3H_3O^+$ (down to C_3O^+). The 55 and 56 peaks are more intense for unsubstituted cyclopentanone than for its methyl-substituted analogs.

(4) m/z = 36–43 u. The most intense peaks in this group are observed at 42, 41, and 39 u and could be assigned to $C_3H_6^+$, $C_3H_5^+$, and $C_3H_3^+$, respectively. The shape of this series of peaks is similar for cyclopentanone and methyl-cyclopentanones, but at 394 nm and 1.5×10^{14} W/cm^2, this group is the weakest for 3-methyl-cyclopentanone.

(5) m/z = 24–29 u. The peaks at 27 and 28 u, which can be assigned to $C_2H_3^+$ and $C_2H_4^+$, respectively, are usually the most intense in this $C_2H_n^+$ (n = 0–5) series.

(6) m/z = 12–16 u. This series of peaks corresponds to the CH_n^+ (n = 0–4) ions, with the CH_3^+ (15 u) and C^+ (12 u) peaks usually being most intense in the group.

(7) m/z = 32 and 18 u. These peaks are not seen in the cyclopentanone spectra, but show significant intensities for methyl-cyclopentanones, especially at 394 nm and at the higher laser intensity. Possible assignments could be CH_4O^+ (O_2^+) and H_2O^+, respectively, where O_2^+ and H_2O^+ might originate from impurities.

(8) m/z = 1 u. Proton peaks are clearly observed for all three molecules at the high laser intensity of 5×10^{14} W/cm^2.

3.3. Theoretical consideration of dissociation mechanisms of the ions

The dissociation mechanism of 2-methyl-cyclopentanone monocation is very complex and many different products can be formed via a variety of competitive channels (Figure 5). The details of the potential energy surface will be described elsewhere. Here, to predict relative product yields at different internal energies of $\mathbf{1}^+$, we carried out RRKM calculations of rate constants for unimolecular isomerization and dissociation steps and then solved the first-order rate equations and computed the branching ratios at E_{int} = 40–300 kcal/mol. At lower energies, the $C_4H_5O^+$ (m/z = 69) + C_2H_5 channel, occurring via the $\mathbf{1}^+ \rightarrow \mathbf{7}^+ \rightarrow \mathbf{8}^+ \rightarrow CH_3C(CO)CH_2^+ + C_2H_5$ mechanism requiring only 38.3 kcal/mol of energy, shows the highest yield. At higher energies, around

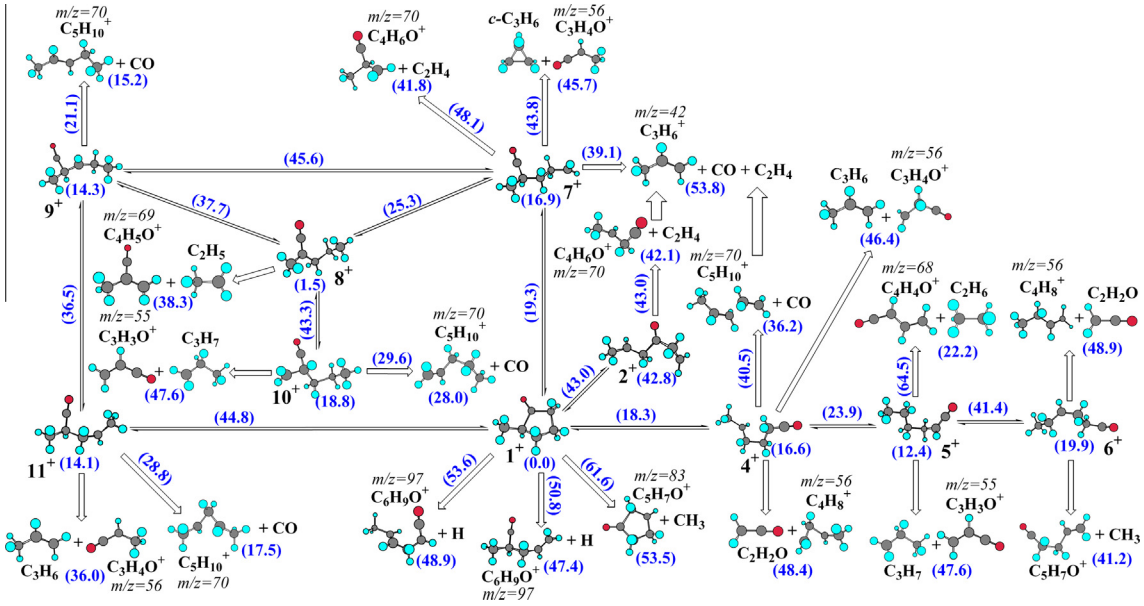

Figure 5. Potential energy graph of various dissociation channels of 2-methyl-cyclopentanone monocation ($\mathbf{1}^+$) calculated at the G3(MP2,CCSD)//B3LYP/6-31G* level of theory. Relative energies (in kcal/mol) of various stable structures and transition states (next to arrows) are given in parentheses.

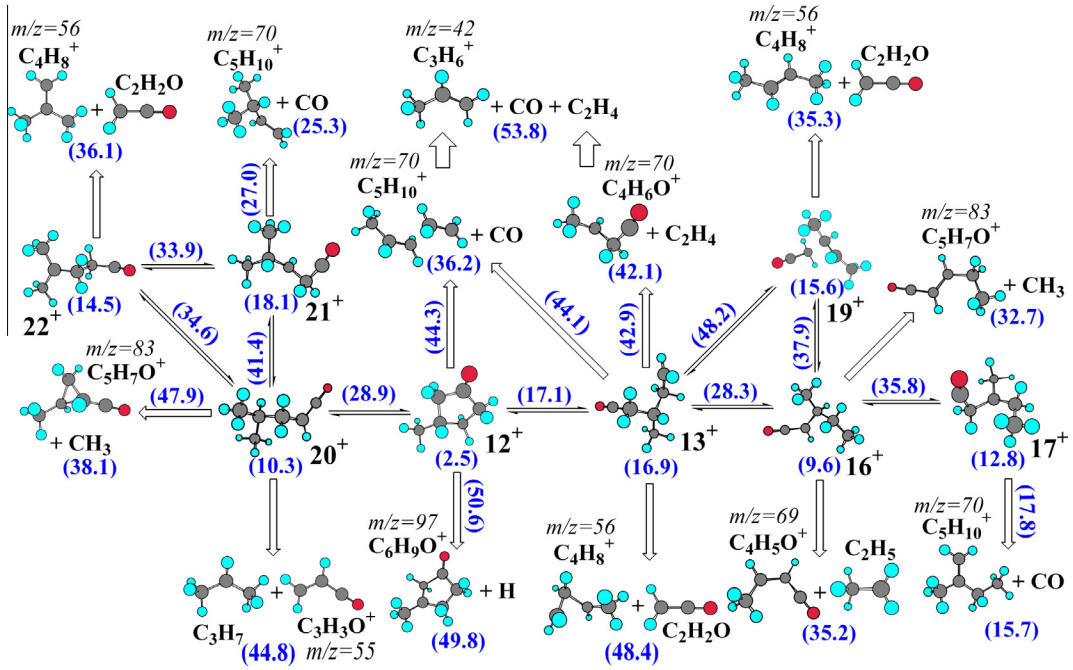

Figure 6. Potential energy graph of various dissociation channels of 3-methyl-cyclopentanone monocation ($\mathbf{12}^+$) calculated at the G3(MP2,CCSD)//B3LYP/6-31G* level of theory. Relative energies (in kcal/mol) of various stable structures and transition states (next to arrows) are given in parentheses.

E_{int} = 70 kcal/mol, the two channels producing m/z = 70 ions, $\mathbf{1}^+ \rightarrow \mathbf{2}^+ \rightarrow CH_3CHCH_2CO^+ + C_2H_4$ and $\mathbf{1}^+ \rightarrow \mathbf{4}^+ \rightarrow C_3H_6^+ \ldots C_2H_4 + CO$ requiring 43.0 and 40.5 kcal/mol of activation energy, respectively, become most important. However, the ions produced in these channels are only weakly bound and would easily decompose as $CH_3CHCH_2CO^+ \rightarrow CH_3CHCH_2^+ + CO$ and $C_3H_6^+ \ldots C_2H_4 \rightarrow CH_3CHCH_2^+ + C_2H_4$, if they have 11.7 and 17.6 kcal/mol in internal energy. Then, the two channels produce the same $C_3H_6^+ + C_2H_4 + CO$ products and are responsible for the m/z = 42 peak. The other two significant channels with branching ratios reaching 20–23% are $C_3H_3O^+$ (m/z = 55) + C_3H_7 occurring via $\mathbf{1}^+ \rightarrow \mathbf{4}^+ \rightarrow \mathbf{5}^+$ and requiring 47.6 kcal/mol as well as $C_4H_8^+$ (m/z = 56) + H_2C_2O (via $\mathbf{4}^+$, 48.4 kcal/mol). At higher energies, another channel producing m/z = 56, $CH_2CH_2CO^+ + C_3H_6$ (via $\mathbf{4}^+$, 46.4 kcal/mol), is also significant. The other products with small but nonzero branching ratios include CH_3CHCO^+ (m/z = 56) + CH_3CHCH_2/c-C_3H_6, $CH_3CH(CO)CH_2^+$ (m/z = 70) + C_2H_4, $C_4H_4O^+$ (m/z = 68) + C_2H_6, $C_5H_7O^+$ (m/z = 83) + CH_3, and $C_6H_9O^+$ (m/z = 97) + H. Thus, the calculations allowed us to explain the appearance of the 55, 56, 69 u peaks and weak 70 and 83 u features in

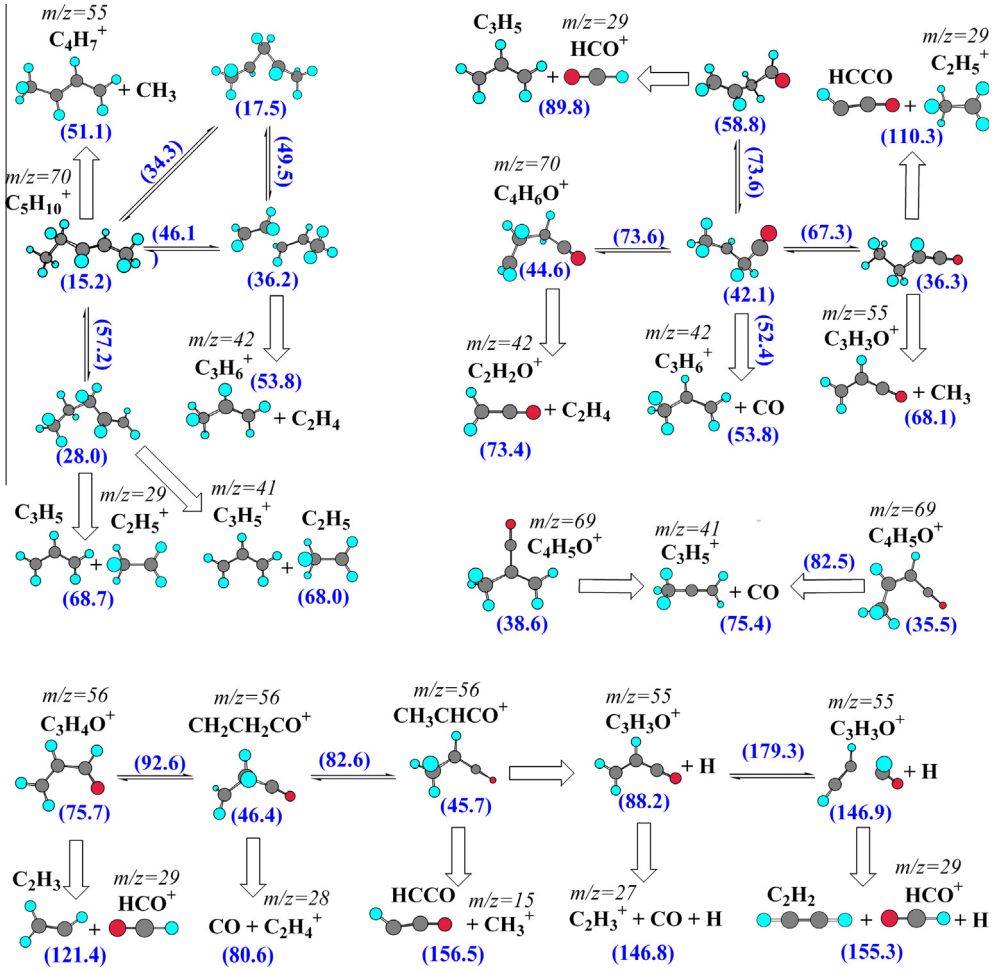

Figure 7. Potential energy graphs of secondary dissociation channels: $C_5H_{10}^+$, $C_4H_6O^+$, $C_4H_5O^+$, $C_3H_4O^+$, and $C_3H_3O^+$. Relative energies (in kcal/mol) of various stable structures and transition states (next to arrows) are given in parentheses.

the mass spectra and also showed that the 42 u peak is likely to originate from secondary decomposition of the weakly bound $m/z = 70$ ions, $CH_3CHCH_2CO^+$ and $C_3H_6^+ \ldots C_2H_4$.

The decomposition mechanism of 3-methyl-cyclopentanone cation is illustrated in Figure 6. According to RRKM calculations, at low E_{int} the main dissociation product pair is expected to be $C_4H_5O^+$ ($m/z = 69$) + C_2H_5 formed via the **12⁺ → 13⁺ → 16⁺** → $CH_3CHCHCO^+ + C_2H_5$ channel. The next important product channel is $C_3H_3O^+$ ($m/z = 55$) + C_3H_7 produced via the **12⁺ → 20⁺** path. This pair has the largest calculated relative yield at E_{int} = 75–140 kcal/mol. At higher energies, the $C_4H_6O^+$ ($m/z = 70$) + C_2H_4 product takes over, which is formed via the **12⁺ → 13⁺** → $CH_3CHCH_2CO^+ + C_2H_4$ pathway. Finally, at internal energies above ~220 kcal/mol, $C_5H_{10}^+$ ($m/z = 70$) + CO formed in the **12⁺ → 13⁺** → $C_3H_6^+ \ldots C_2H_4$ + CO channel becomes the major product pair. Another significant product, up to ~12% at E_{int} around 175–200 kcal/mol, is $CH_2CH_2CHCH_3^+$ ($C_4H_8^+$, $m/z = 56$) + H_2C_2O produced from **13⁺**. In addition, minor and/or trace dissociation products may include $CH_2C(CH_3)_2^+$ ($C_4H_8^+$, $m/z = 56$) + H_2C_2O, $CH_3CH(CH_3)CHCH_2^+$ ($C_5H_{10}^+$, $m/z = 70$) + CO, $CH_3CHCHCH_3^+$ ($C_4H_8^+C_4H_8^+$, $m/z = 56$) + H_2C_2O, $CH_3C(CH_2)CH_2CH_3^+$, ($C_5H_{10}^+$, $m/z = 70$) + CO, $CH_3CH_2CHCHCO^+$ ($C_5H_{10}^+$, $m/z = 70$) + CO, and c-$C_3H_4(CH_3)(CO)^+$ ($C_5H_{10}^+$, $m/z = 70$) + CO. One can see that, similar to 2-methyl-cyclopentanone, the major peaks that may appear in the mass spectra of primary decomposition of 3-methyl cyclopentanone monocation include 55, 56, 69, and 70 u, with a minor contribution of 83 u. These features indeed represent important features of the electron ionization (EI) spectra of 2- and 3-methyl-cyclopntanones [44]. In addition, there is a strong peak at 42 u (in the $C_3H_x^+$ series, 36–43 u) but the 70 u primary products $C_3H_6 \ldots C_2H_4$ and $CH_3CHCH_2CO^+$ are only weakly bound and can easily dissociate to $C_3H_6^+ + C_2H_4$ and $C_3H_6^+ + CO$ giving rise to the 42 u peak. As compared to the EI spectra, the spectra in the intense laser field clearly have the intensity shifted towards smaller fragments and this trend strengthens as the laser intensity increases. The main additional groups of peaks observed correspond to C_2H_x (x = 0–6, 24–30 u) and CH_x^+ (x = 0–4, 12–16 u). They may result from secondary or even deeper dissociation channels.

The secondary decomposition of the major primary fragments of 55 u ($C_3H_3O^+$), 56 u ($C_3H_4O^+$), and 70 u ($C_4H_6O^+$ and $C_5H_{10}^+$) illustrated in Figure 7 can account for the appearance of the $C_3H_x^+$ peaks, with $C_3H_6^+$ of 42 u being the major, and $C_2H_x^+$ peaks (especially, $C_2H_4^+$ (28), $C_2H_5^+$ (29), and $C_2H_3^+$ (27)).

4. Conclusions

The mass spectra obtained in intense laser fields have peak intensities shifted toward smaller fragments as compared to the EI spectra and the trend strengthens with the laser intensity. Secondary decomposition of the major primary fragments $C_5H_{10}^+$ and $C_4H_6O^+$ (70 u) as well as $C_3H_3O^+$ (55 u) and $C_3H_4O^+$ (56 u) can account for the appearance of the $C_3H_x^+$ peaks (with $C_3H_6^+$ of 42 u being the major) and $C_2H_x^+$ peaks ($C_2H_4^+$ (28 u), $C_2H_5^+$ (29 u), and

$C_2H_3^+$ (27 u)) in the mass spectra. Meanwhile, the CH_x^+ group or H^+ could not be attributed to secondary dissociation. These fragments might be formed in principle from 2- and 3-methyl cyclopentanone dications. Our calculations using g-KFR theory indicated that the second photoionization rate constants are several orders of magnitude smaller than those for the first photoionization. However, considering that the laser field intensity is in the range of $3 \times 10^{13} \div 4 \times 10^{14}$ W/cm^2, the kinetic energy of the re-scattering electrons may reach values sufficiently higher than the second ionization potential and thus, dications might be formed via the interaction with the re-scattering electrons [45,46]. Finally, the CH_x^+ and H^+ fragments may also result from dissociation from highly excited electronic levels or from deep sequential decomposition of primary, secondary, and further fragments following the irradiation by the intense laser pulses.

Acknowledgments

Support by National Basic Research Programs of China under Grant No. 2013CB922200 and the National Science Foundation of China (Grant Nos. 11034003, 91221301) is acknowledged. AMM thanks the US DOE (Grant No. DE-FG02-04ER15570) for partial support.

References

[1] C. Kosmidis, J.G. Philis, P. Tzallas, Phys. Chem. Chem. Phys. 1 (1999) 2945.
[2] K. Furuya, E. Yamamoto, Y. Jinbou, T. Ogawa, J. Elec, Spectr. Rel. Phen. 73 (1995) 59.
[3] M. Baba, H. Shinohara, N. Nishi, N. Hirota, Chem. Phys. 83 (1984) 221.
[4] T.J. Cornish, T. Baer, J. Am. Chem. Soc. 109 (1987) 6915.
[5] C. Kosmidis, G. Boulakis, A. Bolovinos, P. Tsekeris, P. Brint, J. Mol. Struct. 266 (1992) 133.
[6] E.W.G. Diau, C. Kotting, T.I. Solling, A.H. Zewail, ChemPhysChem 3 (2002) 57.
[7] E.W.G. Diau, C. Kotting, A.H. Zewail, ChemPhysChem 2 (2001) 273.
[8] C.Y. Wu, Y. Cheng, Y.J. Ziong, J.X. Wang, A.K. Fan, Chin. Chem. Let. 11 (2000) 545.
[9] D. Wu, Q. Wang, X. Cheng, M. Jin, X. Li, Z. Hu, D. Ding, J. Phys. Chem. A 111 (2007) 9494.
[10] Q. Wang, D. Wu, M. Jin, F. Liu, F. Hu, X. Cheng, H. Liu, Z. Hu, D. Ding, H. Mineo, Y.A. Dyakov, A.M. Mebel, S.D. Chao, S.H. Lin, J. Chem. Phys. 129 (2008) 204302.
[11] M. Etinski, C.M. Marian, Phys. Chem. Chem. Phys. 12 (2010) 4915.
[12] C.M. Tseng, Y.T. Lee, C.K. Ni, J. Phys. Chem. A 113 (2009) 3881.
[13] C.K. Lin, C.L. Huang, J.C. Jiang, A.H.H. Chang, Y.T. Lee, S.H. Lin, C.K. Ni, J. Am. Chem. Soc. 124 (2002) 4068.
[14] C.M. Tseng, Y.A. Dyakov, C.L. Huang, A.M. Mebel, S.H. Lin, Y.T. Lee, C.K. Ni, J. Am. Chem. Soc. 126 (2004) 8760.
[15] Z. Yang, M.T. Rodgers, Int. J. Mass Spec. 241 (2005) 225.
[16] K. Chenoweth, C.E. Dykstra, Chem. Phys. Lett. 402 (2005) 329.
[17] Q. Wang, D. Wu, D. Zhang, M. Jin, F. Liu, H. Liu, Z. Hu, D. Ding, H. Mineo, Y.A. Dyakov, Y. Teranishi, S.D. Chao, A.M. Mebel, S.H. Lin, J. Phys. Chem. C 113 (2009) 11805.
[18] M.V. Ammosov, N.B. Delone, V.P. Krainov, Sov. Phys. JETP 64 (1986) 1191.
[19] X.M. Tong, C.D. Lin, J. Phys. 38 (2005) 2593.
[20] L.V. Keldysh, Sov. Phys. JETP 20 (1965) 1307.
[21] K. Mishima, K. Nagaya, M. Hayashi, S.H. Lin, Phys. Rev. A 70 (2004) 063414.
[22] K. Nagaya, H. Mineo, K. Mishima, A.A. Villaeys, M. Hayashi, S.H. Lin, Phys. Rev. A 75 (2007) 013402.
[23] F.H.M. Faisal, J. Phys. B 6 (1973) L89.
[24] H.R. Reiss, Phys. Rev. A 22 (1980) 1786.
[25] T.K. Kjeldsen, C.Z. Bisgaard, L.B. Madsen, H. Stapelfeldt, Phys. Rev. A 68 (2003) 063407.
[26] V.I. Usachenko, S.-I. Chu, Phys. Rev. A 71 (2005) 063410.
[27] H. Mineo, S.D. Chao, K. Nagaya, K. Mishima, M. Hayashi, S.H. Lin, Chem. Phys. Lett. 439 (2007) 224.
[28] K. Mishima, M. Hayashi, J. Yi, S.H. Lin, H.L. Selzle, E.W. Schlag, Phys. Rev. A 66 (2002) 033401.
[29] H. Mineo, K. Nagaya, M. Hayashi, S.H. Lin, J. Phys. B 40 (2000) 2435.
[30] N. Nakashima, T. Yatsuhashi, M. Murakami, R. Mizoguchi, Y. Shimada, in: S.H. Lin, A.A. Villaeys, Y. Fujimura (Eds.), Advances in Multi-photon Processes and Spectroscopy, World Scientific, Singapore, 2006, p. 179.
[31] M. Sharifi, F. Kong, S.L. Chin, H. Mineo, Y. Dyakov, A.M. Mebel, S.D. Chao, M. Hayashi, S.H. Lin, J. Phys. Chem. A 111 (2007) 9405.
[32] P.J. Stephens, F.J. Devlin, C.F. Chabalowski, M.J. Frisch, J. Phys. Chem. 98 (1994) 11623.
[33] A.G. Baboul, L.A. Curtiss, P.C. Redfern, K. Raghavachari, J. Chem. Phys. 110 (1999) 7650.
[34] L.A. Curtiss, K. Raghavachari, Chem. Phys. Lett. 314 (1999) 101.
[35] M.J. Frisch et al., Gaussian 03, REVISION B.03, Gaussian Inc., Pittsburgh, 2003.
[36] MOLPRO is a package of *ab initio* programs written by H.-J. Werner and P.J. Knowles with contributions from J.A. Almlöf, M.J.O. Deegan, S.T. Elbert, C. Hampel, W. Meyer, K. Peterson, R. Pitzer, A.J. Stone, P.R. Taylor, R. Lindh.
[37] T.S. Zyubina, Y.A. Dyakov, S.H. Lin, A.D. Bandrauk, A.M. Mebel, J. Chem Phys. 123 (2005) 134320.
[38] A.M. Mebel, T.S. Zyubina, Y.A. Dyakov, A.D. Bandrauk, S.H. Lin, Int. J. Quantum Chem. 102 (2005) 506.
[39] M.F. Lin, Y.A. Dyakov, S.H. Lin, Y.T. Lee, C.K. Ni, J. Phys. Chem. B 109 (2005) 8344.
[40] Y.A. Dyakov, C.K. Ni, S.H. Lin, Y.T. Lee, A.M. Mebel, J. Phys. Chem. A 109 (2005) 8774.
[41] Y.A. Dyakov, A.M. Mebel, S.H. Lin, Y.T. Lee, C.K. Ni, J. Phys. Chem. A 111 (2007) 9591.
[42] M.F. Lin, Y.A. Dyakov, Y.T. Lee, S.H. Lin, A.M. Mebel, C.K. Ni, J. Chem. Phys. 127 (2007) 064308.
[43] C.K. Ni, C.M. Tseng, M.F. Lin, Y.A. Dyakov, J. Phys. Chem. B 111 (2007) 12631.
[44] P.J. Linstrom, Mallard W.G., in: S.E. Stein (Ed.), NIST Standard Reference Database, 69, National Institute of Standards and Technology, Gaithersburg MD, 2005, p. 20899.
[45] H. Niikura, P.B. Corkum, Adv. Atom. Mol. Opt. Phys. 54 (2007) 511. and references therein.
[46] A.D. Bandrauk, S. Chelkowski, D.J. Diestler, J. Manz, K.-J. Yuan, Int. J. Mass Spec. 277 (2008) 189.